Capacitive and magnetoresistive origin of magnetodielectric effects in Sm-substituted spiral antiferromagnet BiMnFe2O6

Somnath Ghara, Kyongjun Yoo, Kee Hoon Kim, and A. Sundaresan

Citation: Journal of Applied Physics **118**, 164103 (2015); doi: 10.1063/1.4934509
View online: http://dx.doi.org/10.1063/1.4934509
View Table of Contents: http://scitation.aip.org/content/aip/journal/jap/118/16?ver=pdfcov
Published by the AIP Publishing

Capacitive and magnetoresistive origin of magnetodielectric effects in Sm-substituted spiral antiferromagnet $BiMnFe_2O_6$

Somnath Ghara,[1] Kyongjun Yoo,[2] Kee Hoon Kim,[2] and A. Sundaresan[1,a)]
[1]*Chemistry and Physics of Materials Unit, Jawaharlal Nehru Centre for Advanced Scientific Research, Jakkur P.O., Bangalore 560064, India*
[2]*CeNSCMR, Department of Physics and Astronomy, Seoul National University, Seoul 151-747, South Korea*

(Received 14 July 2015; accepted 10 October 2015; published online 26 October 2015)

$BiMnFe_2O_6$ exhibits a spiral antiferromagnetic ordering below 212 K and a reentrant spin glass transition at 34 K. Further, magnetic and dielectric anomalies occur at the same temperature ($T = 170$ K) with a significant magnetodielectric effect. Upon substitution of Sm^{3+} for Bi^{3+} ions in $Bi_{1-x}Sm_xMnFe_2O_6$ ($x = 0.1$ and 0.2), the dielectric anomaly shifts to low temperatures ($T = 135$ and 72 K, respectively), whereas the magnetic anomaly develops into a weak ferromagnetism. For $x = 0.2$, the weak ferromagnetism occurs in a wide temperature range (90–201 K). Below 90 K, it undergoes a transition to an antiferromagnetic state. In contrast to the parent compound ($x = 0$), the magnetodielectric effect is observed both in the antiferromagnetic region ($T < 90$ K) with a maximum at the dielectric anomaly (72 K) and also in the weak ferromagnetic region. It has been shown that the magnetodielectric effect in the antiferromagnetic region has an intrinsic capacitive origin while that observed at the weak ferromagnetic region originates from magnetoresistance. [http://dx.doi.org/10.1063/1.4934509]

Multiferroics have received much attention in the last few decades owing to their fundamental mechanism as well as technological applications.[1–4] Particularly, magnetism-driven ferroelectricity has become important after the discovery of cycloidal spin-induced ferroelectricity in $TbMnO_3$.[5–8] Later, spiral magnetism-driven multiferroicity has been observed in other oxides such as $MnWO_4$, $Ni_3V_2O_8$, $CoCr_2O_4$, and some of the hexaferrites.[9–12] In these materials, a large magnetodielectric effect has been observed due to the presence of magnetoelectric coupling. However, there are some materials such as $YFe_{1-x}Mn_xO_3$, La_2NiMnO_6, and $\gamma-Fe_2O_3$, where a strong magnetodielectric effect is observed without magnetoelectric coupling.[13–15] The origin of this magnetodielectric effect has been suggested to be due to intrinsic capacitive or extrinsic resistive effect.[13,15,16]

Recently, a bismuth based oxide $BiMnFe_2O_6$ with a complex crystal structure has been reported to exhibit very interesting magnetic properties.[17,18] In this material, both Mn^{3+} and Fe^{3+} ions are randomly distributed in two different crystallographic sites, M1 and M2, which form distorted octahedral coordination with oxygen ions. The M1-site octahedra are connected by face, edge, and corner sharing, while the M2-site octahedra are connected only by corner sharing. These two octahedra, M1 and M2, are interconnected by a further complicated arrangement involving corner and edge sharing. Despite such a complex disorder arrangement of magnetic ions, it exhibits a long range spiral magnetic ordering at ~212 K. In addition, a sharp anomaly was reported around 34 K in magnetization. In a recent article, from detailed dc and ac magnetization experiments, it has been shown that the low temperature (34 K) anomaly represents a reentrant spin-glass (RSG) transition caused by the complex crystal structure and disordered Fe^{3+}/Mn^{3+} ions.[19] Below 34 K, both glassy state and long range antiferromagnetic (AFM) ordering coexist, and analysis of magnetization relaxation data reveals the presence of spin-cluster in the reentrant spin-glass state. Further, a magnetization anomaly was reported around 170 K, where a broad frequency-independent dielectric anomaly was also observed with a significant magnetocapacitance effect.[19] Despite the presence of lone pair electrons in Bi^{3+} and the spiral magnetic ordering of Mn^{3+}/Fe^{3+}, $BiMnFe_2O_6$ remains non-ferroelectric because of antipolar arrangement of Bi^{3+} ions and a strong antiferromagnetic coupling of spiral chains along the *c*-direction.[17–19] One possibility to induce ferroelectricity in this compound is to modify the nature of the spiral ordering by substituting rare earth or other transition metal ions for Bi^{3+} or Mn^{3+}/Fe^{3+} ions, respectively. It has already been reported that the substitution of Cr^{3+} at the Mn^{3+} site does not have much effect on the magnetic properties.[20]

In this article, we report results of magnetic and electrical properties of Sm-substituted $BiMnFe_2O_6$. With increasing Sm content in $Bi_{1-x}Sm_xMnFe_2O_6$ ($x = 0.1$ and 0.2), the magnetization and dielectric anomalies, that are observed around 170 K in $x = 0$, separate out and occur at different temperatures. The magnetization anomaly develops into a weak ferromagnetism (WFM) in a broad temperature range (90 K to 201 K) for $x = 0.2$. On the other hand, the dielectric anomaly shifts to lower temperatures and it occurs at 72 K for $x = 0.2$. A magnetocapacitance with capacitive origin is observed in the antiferromagnetic regions ($T < 90$ K) with a maximum around the dielectric anomaly, whereas magnetocapacitance with a butterfly loop is observed in the weak ferromagnetic region where the magnetocapacitance correlates with magnetoresistance. Despite the changes in

a)Author to whom correspondence should be addressed. Electronic mail: sundaresan@jncasr.ac.in

magnetic and dielectric properties, ferroelectricity is not observed in these compounds.

Polycrystalline $Bi_{1-x}Sm_xMnFe_2O_6$ (x = 0, 0.1, and 0.2) samples were prepared by the conventional solid state synthesis method by mixing a stoichiometric amount of Bi_2O_3, Sm_2O_3 (preheated at 900 °C for 12 h), Mn_2O_3, and Fe_2O_3 and heating the mixture at high temperatures. The final sintering temperature was 900 °C, 920 °C, and 940 °C for x = 0, 0.1, and 0.2, respectively. All of these samples were characterized by x-ray diffraction (XRD) method using the PANalytical Empyrean alpha 1 diffractometer with a monochromatized Cu Kα1 radiation. Analysis of the XRD data was carried out by Rietveld refinement with Fullprof software.[21] Low temperature magnetic measurements were carried out in a Superconducting QUantum Interference Device (SQUID, Quantum Design) magnetometer with 3 K/min rate, and high temperature magnetic measurements were performed with 5 K/min rate in Physical Property Measurement System (PPMS, Quantum Design) in an oven mode. The dielectric constant and dielectric loss data were recorded with the heating rate 1 K/min in Agilent E4980A LCR meter with a multifunction probe in PPMS. Resistivity was measured with a Keithley 6517A electrometer using the two-probe method. The conventional *P-E* loop and positive-up-negative-down (PUND) measurements were carried out with a Radiant Technology Precision Workstation and a home-made instrument based on the Sawyer-Tower circuit, respectively.[22]

Single phase samples were obtained up to x = 0.2. XRD patterns obtained from the Rietveld refinement with *Pbcm* space group are shown in Fig. 1. The lattice parameters and volume of the unit cell of all the samples are given in Table I. The lattice parameters *a* and *c* decrease whereas the parameter *b* increases with increasing Sm^{3+} content. Volume (*V*) of the unit cell decreases monotonically with increasing x, which is consistent with the substitution of smaller Sm^{3+} ions (1.079 Å in eight coordination) for Bi^{3+} (1.17 Å in eight coordination) ions.

Figs. 2(a) and 2(b) show the field-cooled-warming (FCW) magnetization measured under a magnetic field of 100 Oe for x = 0 and 0.1, respectively. Fig. 2(c) shows the magnetization measured at the same field for x = 0.2 under field-cooled-cooling (FCC) and FCW conditions. It is to be noted that the long-range magnetic ordering temperature (T_N) decreases from 212 K (x = 0) to 201 K for x = 0.2. The weak magnetic anomaly observed around 170 K in x = 0, as shown in the inset of Fig. 2(a), becomes prominent in Sm-substituted samples even at low magnetic fields as seen in Figs. 2(b) and 2(c). In the case of x = 0.2, it is interesting to note that the magnetization increases rapidly below T_N = 201 K and drops below 165 K. This broad peak between 90 K and 201 K suggests a WFM state which is supported by the results of field dependent magnetization measurements as discussed later. Below 90 K, the weak ferromagnetism disappears and the compound enters into an AFM state. Similar to x = 0, the anomaly due to RSG transition is observed in x = 0.1 and 0.2 as shown in Figs. 2(b) and 2(c). Thus, it is clear from Fig. 2(c) that the sample, x = 0.2, exhibits multiple magnetic states which are highlighted in the same figure. The WFM-AFM transition is so robust that it is not

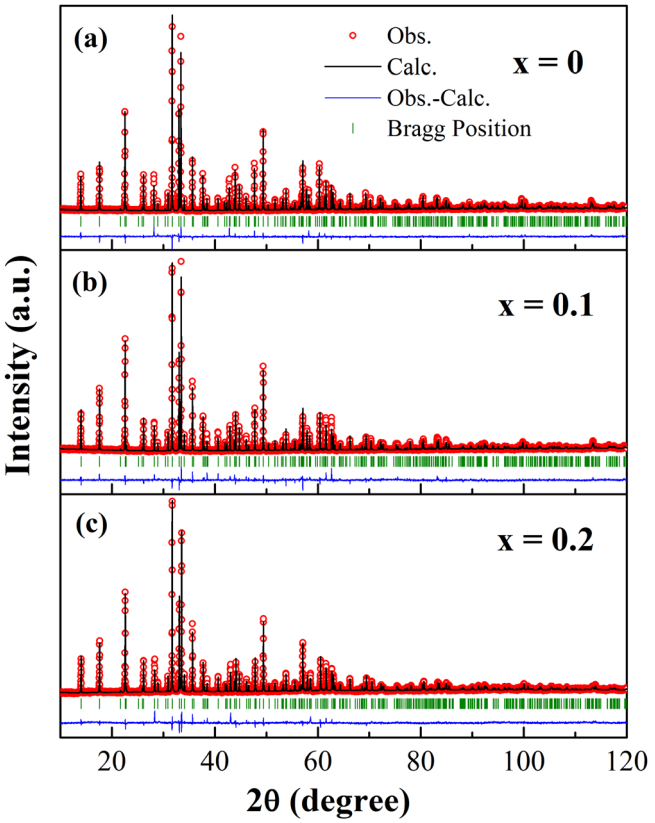

FIG. 1. Room temperature X-ray diffraction patterns of $Bi_{1-x}Sm_xMnFe_2O_6$ (x = 0, 0.1, and 0.2).

suppressed at high magnetic field (70 kOe) as shown in the inset (right) of Fig. 2(c). A clear thermal hysteresis is observed between the FCC and FCW magnetization, as shown in Fig. 2(c), indicating the first order nature of the WFM-AFM transition. To further confirm the first order nature of this transition, we have used the Banerjee criterion to analyze the magnetization data. According to this criterion, a negative slope in the *H*/*M* vs. M^2 plot represents a first order transition.[23,24] *H*/*M* vs. M^2 curves at different temperatures are shown in Fig. 2(d). A clear negative slope of these curves further confirms the first order nature of the transition.

Since neutron diffraction experiments in $BiMnFe_2O_6$ have revealed the presence of a short-range interaction above T_N,[17] we fitted the high temperature (450–600 K) magnetization data well above the Néel temperature with Curie-Weiss law and the results are shown in Fig. 2(e) and the parameters obtained from the fitting are given in Table I. For x = 0, the obtained value for the Curie-Weiss temperature (θ_{CW}) is −890 K which is much higher than the Néel temperature (T_N = 212 K), and the frustration parameter *f* (= $|\theta_{CW}|/T_N$ = 4.2) indicates that the magnetic interaction is moderately frustrated.[19] For the sample, x = 0.2, the Curie-Weiss temperature (θ_{CW}) becomes −1111 K and the frustration parameter (*f*) increases to 5.52. This indicates that Sm substitution leads to more frustrated magnetic interactions. For x = 0 and 0.1, the experimental effective paramagnetic (PM) moment (μ_{exp}) remains very close to the calculated value (μ_{cal}), but for x = 0.2, the μ_{exp} is slightly higher than the μ_{cal}.

The temperature-dependent dielectric constant of all the samples measured with 50 kHz is shown in Fig. 3. In the

TABLE I. Structural and magnetic parameters of $Bi_{1-x}Sm_xMnFe_2O_6$ (x = 0, 0.1, and 0.2).

	Structural parameters				Magnetic parameters				
Sm content	a (Å)	b (Å)	c (Å)	V (Å^3)	T_N (K)	θ_{CW} (K)	$f(\lvert\theta_{CW}\rvert/T_N)$	μ_{cal} (μ_B/f.u.)	μ_{exp} (μ_B/f.u.)
$x=0$	5.03247 (4)	7.06896 (5)	12.66345 (9)	450.493 (6)	212	−890 K	4.20	9.695	9.895
$x=0.1$	5.03194 (6)	7.06999 (8)	12.63157 (14)	449.378 (9)	204	−910 K	4.46	9.707	10.099
$x=0.2$	5.03129 (7)	7.07080 (10)	12.59909 (16)	448.216 (10)	201	−1111 K	5.52	9.718	10.715

x = 0 sample, a broad dielectric anomaly is observed around the weak magnetic anomaly ($T \sim 170$ K).[19] It is to be mentioned that a significant magnetocapacitance has been reported only around the dielectric anomaly.[19] With Sm substitution, this broad dielectric anomaly shifts to lower temperatures, 135 K and 72 K for x = 0.1 and 0.2, respectively. The temperature of the dielectric anomaly is independent of frequency, as shown in the inset of Fig. 3, and correspondingly there is no anomaly in the dielectric loss data (not shown). This indicates that the broad dielectric anomaly is not associated with relaxation phenomena.

In Fig. 4, we show a correlation between the magnetization with magnetocapacitance and magnetoresistance for the sample with x = 0.2. Magnetic field dependent magnetization data measured at different temperatures are shown in Fig. 4(a). The M vs. H curve at 220 K is linear which is consistent with the PM state. On the other hand, a clear hysteresis loop but without saturation is observed at $T = 130$, 165, and 185 K, which shows the presence of a WFM state, whereas a linear behavior observed at 72 K indicates an AFM state. These results, along with the M (T) behavior (Fig. 2(c)), confirm that the weak ferromagnetism exists in a broad temperature range (90 K to 201 K) and disappears below 90 K. The derivative of M (H) with respect to H is shown in Fig. 4(b) where the peak position corresponds to a change in slope of the $M(H)$ curve as seen in Fig. 4(a).

Magnetocapacitance data at different temperatures are shown in Fig. 4(c). In contrast to the parent compound, where magnetocapacitance is observed only around the magnetic/dielectric anomaly, magnetocapacitance in the Sm-substituted

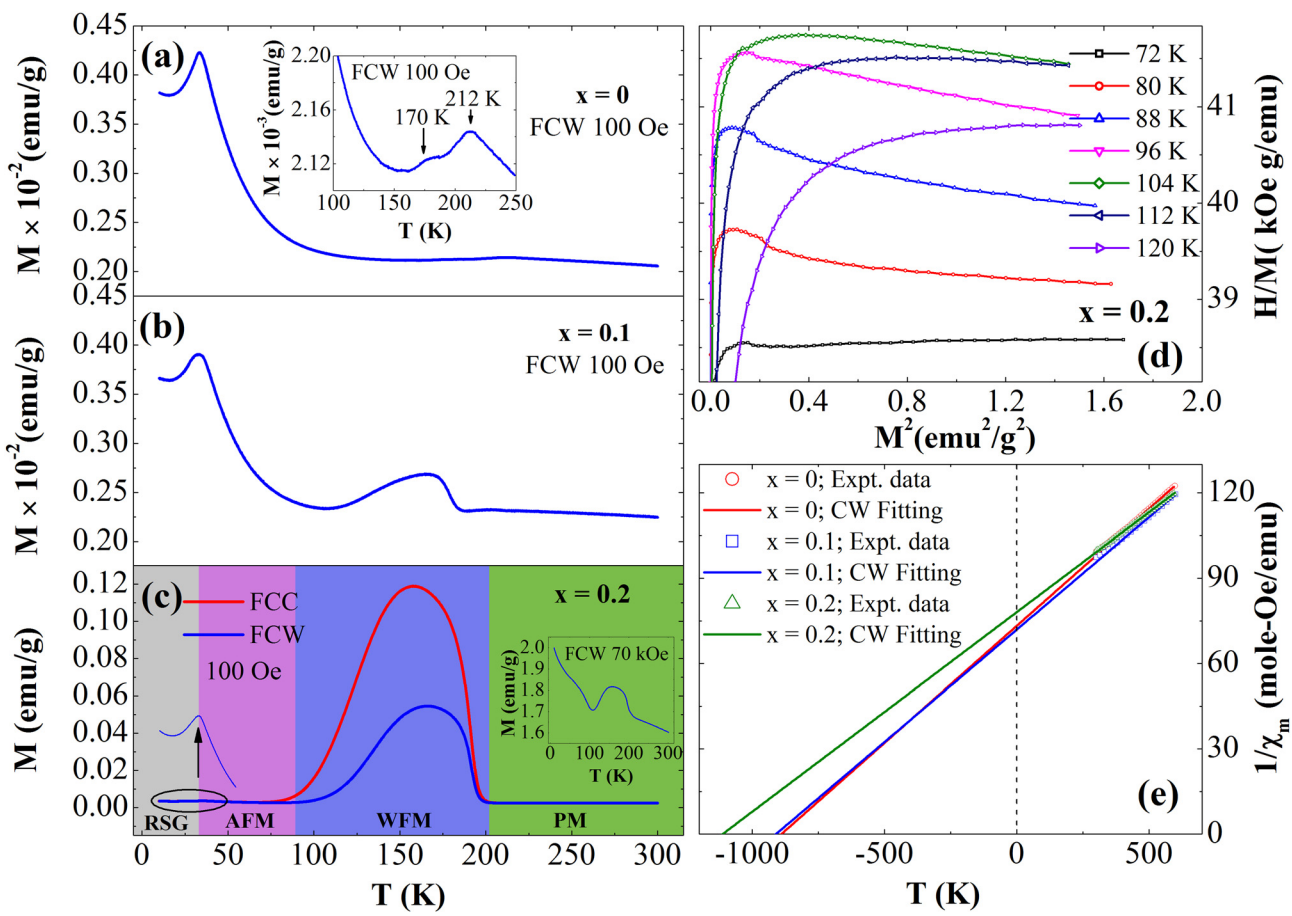

FIG. 2. (a) and (b) Temperature dependent field-cooled-warming (FCW) magnetization under an applied magnetic field of 100 Oe of x = 0 and 0.1 in $Bi_{1-x}Sm_xMnFe_2O_6$, respectively. The inset in Fig. 2(a) shows the weak magnetic anomaly observed around 170 K. (c) Temperature dependent field-cooled-cooling (FCC) and FCW magnetization at the same field in x = 0.2. The left inset shows the reentrant spin-glass transition around 34 K, and the right inset shows FCW magnetization under an applied field of 70 kOe. The different magnetic regions are shown in different colors. (d) H/M vs. M^2 at different temperature indicating the first order nature of the weak ferromagnetic (WFM) to antiferromagnetic (AFM) transition using the Banerjee criterion. (e) $1/\chi_m$ vs. T plot showing the Curie-Weiss behavior in the temperature range 450 K–600 K of $Bi_{1-x}Sm_xMnFe_2O_6$ (x = 0, 0.1, and 0.2).

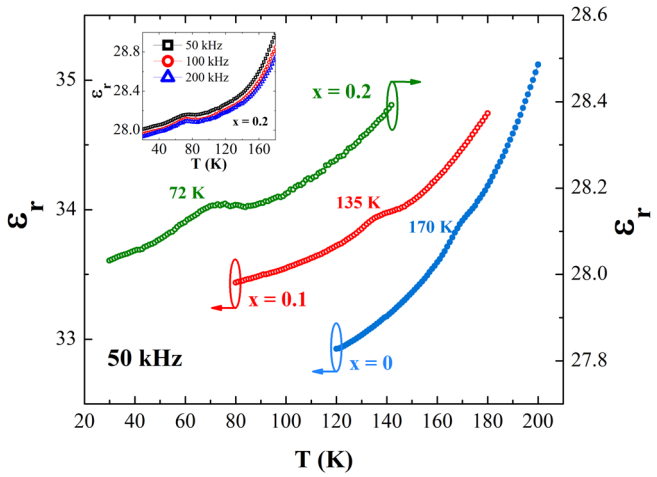

FIG. 3. Temperature dependent dielectric constant measured with 50 kHz of $Bi_{1-x}Sm_xMnFe_2O_6$ (x = 0, 0.1, and 0.2). The inset shows the temperature dependent dielectric constant of the x = 0.2 sample measured at different frequencies.

sample (x = 0.2) is observed in the entire temperature range below $T_N = 201$ K. However, the nature and origin of magnetocapacitance are different in the AFM and WFM states. Magnetocapacitance is observed without any hysteresis in the AFM region (<90 K) including the spin-glass state with a maximum around the dielectric anomaly (72 K). On the other hand, the magnetocapacitance is observed in the WFM region with a butterfly-hysteresis loop. It should be noticed that the kink of the butterfly loop in the magnetocapacitance corresponds to the change in slope of $M(H)$ curves or the peak in dM/dH, as indicated by the vertical dotted lines in Fig. 4. This one-to-one-correspondence between magnetic field dependent magnetization and capacitance as well as the presence of non-zero magnetocapacitance in the AFM region indicate the presence of strong coupling between magnetic and dielectric properties.

To find out whether the observed magnetodielectric effect is intrinsic or extrinsic, we have measured magnetic field dependent resistivity at each temperature. Interestingly, we found that resistivity varies with magnetic field in the WFM region indicating the presence of magnetoresistance. However, below and above the WFM region, resistivity is independent of magnetic field. Thus, the appearance of magnetoresistance is consistent with the weak ferromagnetism. Magnetic field dependent resistivity ρ (H) data are shown in Fig. 4(d). In the WFM region, ρ (H) curves show the typical hysteresis loop. Corresponding to the kink in magnetocapacitance, there is a minimum in ρ (H) curves which indicates that the butterfly-loop observed in the magnetocapacitance is related to the hysteresis in magnetoresistance. On the other hand, the magnetocapacitance observed in the AFM region is not associated with the magnetoresistance. This suggests

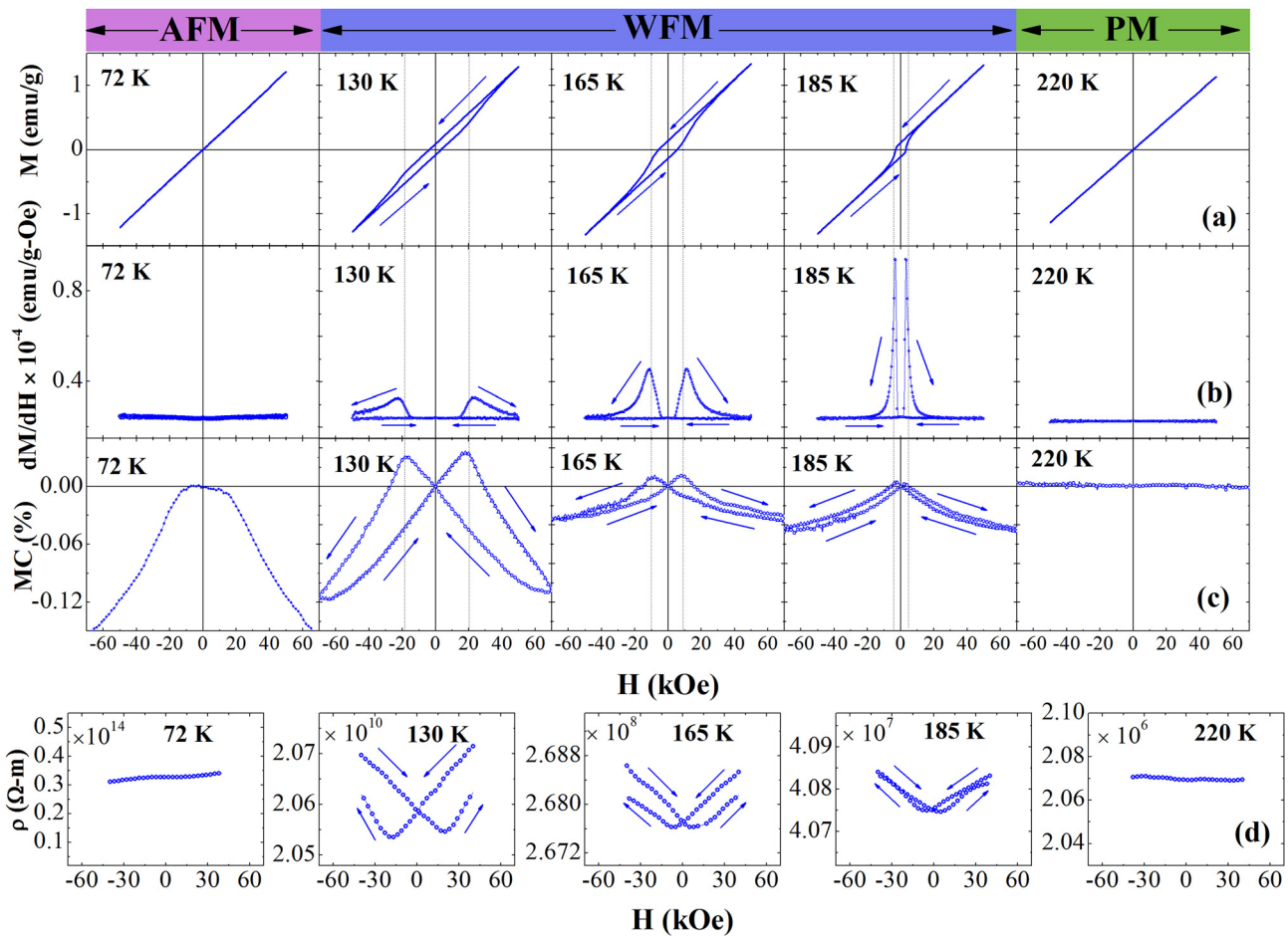

FIG. 4. Magnetic field dependent (a) magnetization (M), (b) dM/dH, and (c) magnetocapacitance (MC%) with 200 kHz, and (d) resistivity (ρ) measured at different temperatures in x = 0.2.

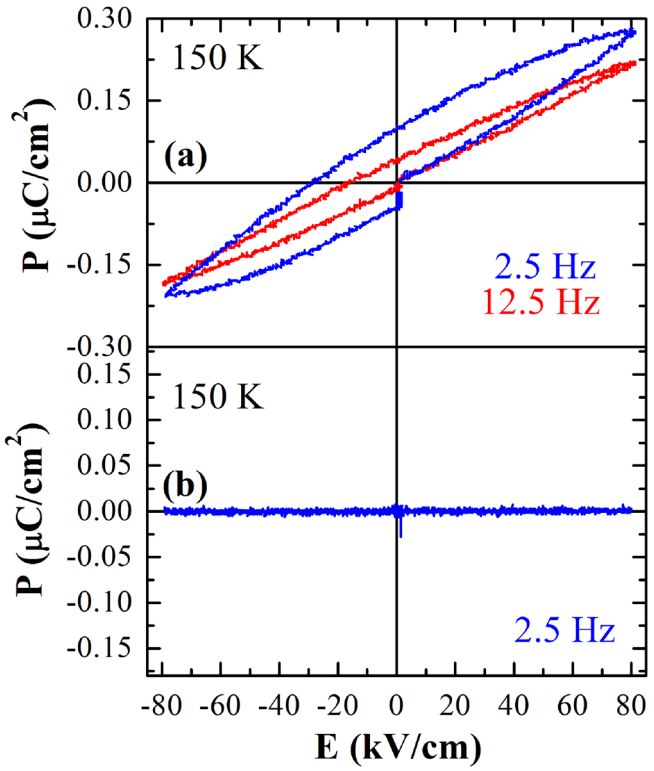

FIG. 5. (a) Conventional *P-E* loop and (b) *P-E* loop obtained from the positive-up-negative-down (PUND) method measured at 150 K in the sample of $x = 0.2$.

that the magnetodielectric effect in the AFM region originates from an intrinsic capacitive contribution, but in the WFM region it is mainly governed by the magnetoresistance. Since the average structure of these samples remain the same, it is not clear how the Sm substitution induces changes in the magnetic and electrical properties of these samples. It requires further study to know whether there is any role of Sm-4f and Mn/Fe-3d moment interactions in inducing these changes.

To probe whether the change in magnetism induces ferroelectricity or not, we have performed *P-E* loop and PUND measurements at 150 K and the results are shown in Figs. 5(a) and 5(b), respectively. The conventional *P-E* loop shows a hysteresis loop resembling the leaky behavior, and the *P-E* loop obtained from the PUND measurement does not show any noticeable ferroelectric polarization at 150 K. PUND measurements performed at 50 K (not shown) also show similar non-ferroelectric behavior. Although there is a change in magnetism upon substitution of Sm-ions, the absence of ferroelectricity requires an understanding of magnetic structure in this compound.

In conclusion, we have shown that the substitution of Sm in $Bi_{1-x}Sm_xMnFe_2O_6$ ($x = 0.1$ and 0.2) induces changes in magnetic and dielectric properties, however, there is no ferroelectricity in these compounds. For $x = 0.2$, a weak ferromagnetism is induced in a wide temperature range (90–201 K), and an antiferromagnetic state exists below 90 K with a dielectric anomaly around 72 K. An intrinsic magnetodielectric effect has been observed in the antiferromagnetic regions with a maximum around the dielectric anomaly. A magnetodielectric effect is also observed in the weak ferromagnetic region with a butterfly hysteresis loop. The origin of this butterfly hysteresis loop has been attributed to the presence of magnetoresistance. Our results demonstrate that the system, $Bi_{1-x}Sm_xMnFe_2O_6$ ($x = 0.1$ and 0.2), is an example of a different origin of the magnetodielectric effect in the same material.

S.G. and A.S. would like to acknowledge Shiek Saqr Laboratory at Jawaharlal Nehru Centre for Advanced Scientific Research for providing experimental facilities. The experimental work at SNU was supported by the National Creative Research Initiative (2010-0018300).

[1]D. Khomskii, Physics **2**, 20 (2009).
[2]S.-W. Cheong and M. Mostovoy, Nat. Mater. **6**, 13 (2007).
[3]N. A. Spaldin, S.-W. Cheong, and R. Ramesh, Phys. Today **63**(10), 38 (2010).
[4]J. Scott, J. Mater. Chem. **22**, 4567 (2012).
[5]T. Kimura, T. Goto, H. Shintani, K. Ishizaka, T. Arima, and Y. Tokura, Nature **426**, 55 (2003).
[6]T. Kimura, Annu. Rev. Mater. Res. **37**, 387 (2007).
[7]Y. Tokura and S. Seki, Adv. Mater. **22**, 1554 (2010).
[8]Y. Tokura, S. Seki, and N. Nagaosa, Rep. Prog. Phys. **77**, 076501 (2014).
[9]K. Taniguchi, N. Abe, T. Takenobu, Y. Iwasa, and T. Arima, Phys. Rev. Lett. **97**, 097203 (2006).
[10]G. Lawes, A. B. Harris, T. Kimura, N. Rogado, R. J. Cava, A. Aharony, O. Entin-Wohlman, T. Yildirim, M. Kenzelmann, C. Broholm, and A. P. Ramirez, Phys. Rev. Lett. **95**, 087205 (2005).
[11]Y. Yamasaki, S. Miyasaka, Y. Kaneko, J. P. He, T. Arima, and Y. Tokura, Phys. Rev. Lett. **96**, 207204 (2006).
[12]T. Kimura, Annu. Rev. Condens. Matter Phys. **3**, 93 (2012).
[13]P. Mandal, V. S. Bhadram, Y. Sundarayya, C. Narayana, A. Sundaresan, and C. N. R. Rao, Phys. Rev. Lett. **107**, 137202 (2011).
[14]D. Choudhury, P. Mandal, R. Mathieu, A. Hazarika, S. Rajan, A. Sundaresan, U. V. Waghmare, R. Knut, O. Karis, P. Nordblad, and D. D. Sarma, Phys. Rev. Lett. **108**, 127201 (2012).
[15]T. Bonaedy, Y. Koo, K. Sung, and J. Jung, Appl. Phys. Lett. **91**, 132901 (2007).
[16]G. Catalan, Appl. Phys. Lett. **88**, 102902 (2006).
[17]T. Yang, A. M. Abakumov, J. Hadermann, G. Van Tendeloo, I. Nowik, P. W. Stephens, J. Hemberger, A. A. Tsirlin, K. V. Ramanujachary, S. Lofland, M. Croft, A. Ignatov, J. Sun, and M. Greenblatt, Chem. Sci. **1**, 751 (2010).
[18]A. M. Abakumov, A. A. Tsirlin, J. M. Perez-Mato, V. Petříček, H. Rosner, T. Yang, and M. Greenblatt, Phys. Rev. B **83**, 214402 (2011).
[19]S. Ghara, B.-G. Jeon, K. Yoo, K. H. Kim, and A. Sundaresan, Phys. Rev. B **90**, 024413 (2014).
[20]D. Batuk, C. De Dobbelaere, A. A. Tsirlin, A. M. Abakumov, A. Hardy, M. K. Van Bael, M. Greenblatt, and J. Hadermann, Mater. Res. Bull. **48**, 2993 (2013).
[21]H. Rietveld, J. Appl. Crystallogr. **2**, 65 (1969).
[22]M. Fukunaga and Y. Noda, J. Phys. Soc. Jpn. **77**, 064706 (2008).
[23]S. K. Banerjee, Phys. Lett. **12**, 16 (1964).
[24]J. Mira, J. Rivas, F. Rivadulla, C. Vázquez-Vázquez, and M. A. López-Quintela, Phys. Rev. B **60**, 2998 (1999).